

# Synthesis and X-ray Structural Characterization of Ru(PPh<sub>3</sub>)<sub>3</sub>(CO)(C<sub>2</sub>H<sub>4</sub>) and RuH(*o*-C<sub>6</sub>H<sub>4</sub>C(O)CH<sub>3</sub>)(PPh<sub>3</sub>)<sub>2</sub>L (L = PPh<sub>3</sub>, CO, DMSO): Ruthenium Complexes with Relevance to the Murai Reaction<sup>†</sup>

Rodolphe F. R. Jazzar, Mary F. Mahon, and Michael K. Whittlesey\*

Department of Chemistry, University of Bath, Claverton Down, Bath BA2 7AY, U.K.

Received May 14, 2001

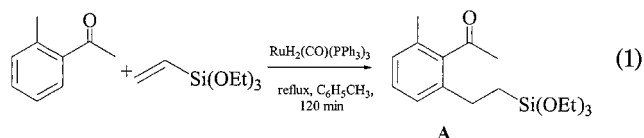
The ruthenium complexes Ru(PPh<sub>3</sub>)<sub>3</sub>(CO)(C<sub>2</sub>H<sub>4</sub>) (**1**) and RuH(*o*-C<sub>6</sub>H<sub>4</sub>C(O)CH<sub>3</sub>)(L)(PPh<sub>3</sub>)<sub>2</sub> (**2**, L = PPh<sub>3</sub>; **3**, L = CO; **4**, L = DMSO) have been prepared in order to assess their activity for catalyzing the insertion of alkenes into the ortho C–H bond of aromatic ketones (Murai reaction). Treatment of RuH<sub>2</sub>(CO)(PPh<sub>3</sub>)<sub>3</sub> with ethene in refluxing toluene afforded **1**, which has been characterized by multinuclear NMR spectroscopy and X-ray crystallography. Excess acetophenone reacted with Ru(H<sub>2</sub>)H<sub>2</sub>(PPh<sub>3</sub>)<sub>3</sub> to give RuH(*o*-C<sub>6</sub>H<sub>4</sub>C(O)CH<sub>3</sub>)(PPh<sub>3</sub>)<sub>3</sub> (**2**), which loses triphenylphosphine upon addition of CO or DMSO to give RuH(*o*-C<sub>6</sub>H<sub>4</sub>C(O)CH<sub>3</sub>)(CO)(PPh<sub>3</sub>)<sub>2</sub> (**3**) and RuH(*o*-C<sub>6</sub>H<sub>4</sub>C(O)CH<sub>3</sub>)(DMSO)(PPh<sub>3</sub>)<sub>2</sub> (**4**), respectively. The X-ray crystal structures of both of these compounds have been determined. The activity for catalyzing the reaction of 2'-methylacetophenone with triethoxyvinylsilane follows the order RuH<sub>2</sub>(CO)(PPh<sub>3</sub>)<sub>3</sub> > **2** > **1** > **4**. Complex **3**, along with both RuH<sub>2</sub>(CO)(AsPh<sub>3</sub>)<sub>3</sub> and RuH<sub>2</sub>(CO)(dppp)(PPh<sub>3</sub>) (dppp = Ph<sub>2</sub>P(CH<sub>2</sub>)<sub>3</sub>PPh<sub>2</sub>), show essentially zero catalytic activity.

## Introduction

There is significant interest in the activation and functionalization of carbon–hydrogen bonds using transition-metal complexes.<sup>1</sup> While considerable progress has been made in understanding the kinetics, thermodynamics, and mechanisms of stoichiometric C–H bond activation reactions,<sup>2</sup> there are still very few examples of catalytic processes involving C–H bond cleavage that result in functionalization.<sup>3</sup> Indeed, the development of a catalytic cycle for the transformation of alkanes has

been described as one of the remaining “Holy Grails” of inorganic chemistry.<sup>4</sup>

In 1993, Murai and co-workers reported a rare example of catalytic C–C bond formation following C–H activation of an aromatic ketone.<sup>5</sup> The reaction of 2'-methylacetophenone with triethoxyvinylsilane in refluxing toluene at 135 °C in the presence of catalytic amounts of RuH<sub>2</sub>(CO)(PPh<sub>3</sub>)<sub>3</sub> gave exclusively the ortho-alkylated product A in 99% yield (eq 1).



It is proposed that this remarkable regioselectivity for activation  $\alpha$  to the ketone group on the aromatic ring arises from coordination of the carbonyl group to the ruthenium (intermediate B, Scheme 1). This places the ortho C–H close to the metal center, where it is activated forming the orthometalated complex C. The importance of these species on the catalytic pathway has been confirmed by density functional calculations.<sup>6</sup>

Other features of the above mechanism are of interest. Alkene hydrogenation by RuH<sub>2</sub>(CO)(PPh<sub>3</sub>)<sub>3</sub> leads to the

\* To whom correspondence should be addressed. E-mail: chsmkw@bath.ac.uk.

<sup>†</sup> Dedicated to Dr. Roger Mawby on the occasion of his retirement.

(1) Jones, W. D. In *Topics in Organometallic Chemistry: Activation of Unreactive Bonds and Organic Synthesis*; Murai, S., Ed.; Springer-Verlag: New York, 1999. Guari, Y.; Sabo-Etienne, S.; Chaudret, B. *Eur. J. Inorg. Chem.* **1999**, 1047.

(2) Representative examples: (a) Shilov, A. E.; Shul'pin, G. B. *Chem. Rev.* **1997**, *97*, 2879. (b) Bromberg, S. E.; Yang, H.; Asplund, M. C.; Lian, T.; McNamara, B. K.; Kotz, K. T.; Yeston, T. S.; Wilkens, M.; Frei, H.; Bergman, R. G.; Harris, C. B. *Science* **1997**, *278*, 260. (c) Bennett, J. L.; Wolczanski, P. T. *J. Am. Chem. Soc.* **1997**, *119*, 10696. (d) Waltz, K. M.; Muhoro, C. N.; Hartwig, J. F. *Organometallics* **1999**, *18*, 3383. (e) Heiberg, H.; Johansson, L.; Gropen, O.; Ryan, O. B.; Swang, O.; Tilset, M. *J. Am. Chem. Soc.* **2000**, *122*, 10831.

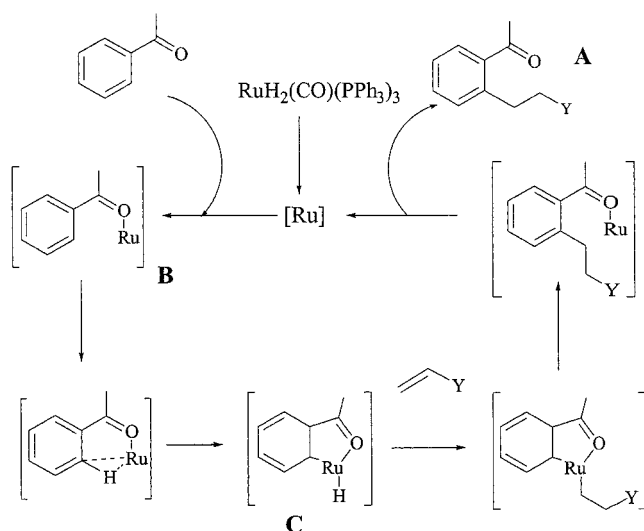
(3) (a) Dyker, G. *Angew. Chem., Int. Ed.* **1999**, *38*, 1699. (b) Kakiuchi, F.; Murai, S. In *Topics in Organometallic Chemistry: Activation of Unreactive Bonds and Organic Synthesis*; Murai, S., Ed.; Springer-Verlag: New York, 1999. (c) Waltz, K. M.; Hartwig, J. F. *Science* **1997**, *277*, 211. (d) Jordan, R. F.; Taylor, D. F. *J. Am. Chem. Soc.* **1989**, *111*, 778. (e) Moore, E. J.; Pretzer, W. R.; O'Connell, T. J.; Harris, J.; Labounty, L.; Chou, L.; Grimmer, S. S. *J. Am. Chem. Soc.* **1989**, *114*, 5888. (f) Lim, Y.-G.; Kim, Y. H.; Kang, J.-B. *Chem. Commun.* **1994**, 2267. (g) Chatani, N.; Fukuyama, T.; Kakiuchi, F.; Murai, S. *J. Am. Chem. Soc.* **1996**, *118*, 493. (h) Periana, R. A.; Taube, D. J.; Gamble, S.; Taube, H.; Satoh, T.; Fujii, H. *Science* **1998**, *280*, 560. (i) Lenges, C. P.; Brookhart, M. *J. Am. Chem. Soc.* **1999**, *121*, 6616. (j) Jia, C.; Piao, D.; Oyamada, J.; Lu, W.; Kitamura, T.; Fujiwara, Y. *Science* **2000**, *287*, 1992. (k) Chen, H.; Schlecht, S.; Simple, T. C.; Hartwig, J. F. *Science* **2000**, *287*, 1995. (l) Jun, C. H.; Hong, J. B.; Kim, Y. H.; Chung, K. Y. *Angew. Chem., Int. Ed.* **2000**, *39*, 3440.

(4) Arndtsen, B. A.; Bergman, R. G.; Mobley, T. A.; Peterson, T. H. *Acc. Chem. Res.* **1995**, *28*, 154.

(5) (a) Murai, S.; Kakiuchi, F.; Sekine, S.; Tanaka, Y.; Kamatani, A.; Sonoda, M.; Chatani, N. *Nature* **1993**, *366*, 529. (b) Murai, S.; Kakiuchi, F.; Sekine, S.; Tanaka, Y.; Kamatani, A.; Sonoda, M.; Chatani, N. *Pure Appl. Chem.* **1994**, *66*, 1527. (c) Kakiuchi, F.; Sekine, S.; Tanaka, Y.; Kamatani, A.; Sonoda, M.; Chatani, N.; Murai, S. *Bull. Chem. Soc. Jpn.* **1995**, *68*, 62. (d) Murai, S.; Chatani, N.; Kakiuchi, F. *Pure Appl. Chem.* **1997**, *69*, 589.

(6) Matsubara, T.; Koga, N.; Musaev, D. G.; Morokuma, K. *J. Am. Chem. Soc.* **1998**, *120*, 12692. Matsubara, T.; Koga, N.; Musaev, D. G.; Morokuma, K. *Organometallics* **2000**, *19*, 2318.

Scheme 1



catalytically active fragment [Ru], which is postulated as a 14- or 16-electron species such as  $\text{Ru}(\text{PPh}_3)_3$  or  $\text{Ru}(\text{CO})(\text{PPh}_3)_3$ . This coordinatively unsaturated fragment would be rapidly trapped in the presence of alkene to afford a ruthenium(0) alkene complex, and indeed, treatment of  $\text{RuH}_2(\text{CO})(\text{PPh}_3)_3$  with a stoichiometric amount of styrene and *o*-acetylstyrene affords the zerovalent species  $[\text{Ru}\{\text{CH}_3\text{C}(\text{O})\text{C}_6\text{H}_4\text{CH}=\text{CH}_2\}(\text{CO})(\text{PPh}_3)_2]$ , in which both the C=O and C=C groups are bonded to the metal center.<sup>7</sup> Related alkene and diene complexes have also been spectroscopically characterized.<sup>8</sup> Dissociation of  $\text{Ru}(\text{CO})(\text{PPh}_3)_n(\text{alkene})$  then occurs in the next step to provide a vacant site for ketone binding prior to C–H activation, although it is still uncertain as to what other ligands are also coordinated to the metal. Calculations on the activation of benzaldehyde by  $\text{Ru}(\text{CO})(\text{PPh}_3)_3$  and  $\text{Ru}(\text{CO})(\text{PPh}_3)_2$  indicate that only the 14-electron complex displays any selectivity for ortho cleavage of the C–H bond.<sup>6</sup>

Chaudret and co-workers have recently demonstrated that  $\text{RuH}_2(\text{H}_2)_2(\text{PCy}_3)_2$  catalyzes the reaction of ethene with acetophenone or benzophenone at room temperature.<sup>9</sup> The ortho-metallated species  $\text{RuH}(\eta^2\text{-H}_2)(o\text{-C}_6\text{H}_4\text{C}(\text{O})\text{CH}_3)(\text{PCy}_3)_2$  also functions as a catalyst under these same mild conditions, indicating further the importance of orthometallated species on the catalytic pathway. In contrast,  $\text{RuH}(o\text{-C}_6\text{H}_4\text{C}(\text{O})\text{CH}_3)(\text{CO})(\text{PCy}_3)_2$  shows no catalytic activity.

We were interested in studying the catalytic activity of ortho-metallated ruthenium complexes containing  $\text{PPh}_3$  groups, to allow direct comparisons with the work of Murai. We have prepared a series of complexes,  $\text{RuH}(o\text{-C}_6\text{H}_4\text{C}(\text{O})\text{CH}_3)(\text{L})(\text{PPh}_3)_2$  ( $\text{L} = \text{PPh}_3, \text{CO}, \text{DMSO}$ ), to probe the effect of the coordinated ligand set on the activity. In addition, we have synthesized and structurally characterized for the first time the zerovalent ethene complex  $\text{Ru}(\text{PPh}_3)_3(\text{CO})(\text{C}_2\text{H}_4)$ .

(7) (a) Lu, P.; Paulasaari, J.; Jin, K.; Bau, R.; Weber, W. P. *Organometallics* **1998**, *17*, 584. (b) Paulasaari, J.; Moiseeva, N.; Bau, R.; Weber, W. P. *J. Organomet. Chem.* **1999**, *587*, 299.

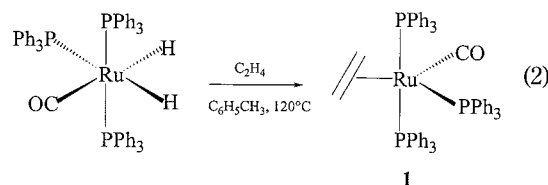
(8) (a) Hiraki, H.; Kira, S.; Kawano, H. *Bull. Chem. Soc. Jpn.* **1997**, *70*, 1583. (b) Hiraki, H.; Ishimoto, T.; Kawano, H. *Bull. Chem. Soc. Jpn.* **2000**, *73*, 2099.

(9) Guari, Y.; Sabo-Etienne, S.; Chaudret, B. *J. Am. Chem. Soc.* **1998**, *120*, 4228. Busch and Leitner have reported very similar results: Busch, S.; Leitner, W. *Chem. Commun.* **1999**, 2305.

## Results and Discussion

**Synthesis and X-ray Crystal Structure of  $\text{Ru}(\text{PPh}_3)_3(\text{CO})(\text{C}_2\text{H}_4)$  (**1**).** The stoichiometric reaction of  $\text{RuH}_2(\text{CO})(\text{PPh}_3)_3$  with  $\text{CH}_2=\text{CHSi}(\text{OMe})_3$  in refluxing toluene at 135 °C was reported to give the hydrogenation product trimethoxyethylsilane, although the fate of the remaining ruthenium fragment was not established.<sup>5</sup> Hiraki et al. have shown reaction of the dihydride complex with an excess of the same alkene leads to Si–OEt cleavage, giving methane, ethane,  $\text{Ru}(\text{PPh}_3)_3(\text{CO})_2$ , and the cyclometalated complex  $\text{RuH}(\text{C}_6\text{H}_4\text{PPh}_2)(\text{PPh}_3)_2(\text{CO})$ . Upon reaction of  $\text{RuH}_2(\text{CO})(\text{PPh}_3)_3$  with an excess of styrene, the bis(styrene) complex  $\text{Ru}(\text{CO})(\text{CH}_2=\text{CHPh})_2(\text{PPh}_3)_2$  was identified as the major product by NMR spectroscopy.<sup>8</sup>

When we treated  $\text{RuH}_2(\text{CO})(\text{PPh}_3)_3$  with ethene in toluene at 120 °C, ethane was produced and a yellow microcrystalline product was formed, which we have identified as  $\text{Ru}(\text{PPh}_3)_3(\text{CO})(\text{C}_2\text{H}_4)$  **1** (eq 2). This com-



pound displayed a single band in the carbonyl region of the IR spectrum at 1854  $\text{cm}^{-1}$ , consistent with a ruthenium(0) oxidation state. Both the  $^{31}\text{P}\{^1\text{H}\}$  and  $^1\text{H}$  NMR spectra indicate that **1** is stereochemically non-rigid at room temperature, analogous to other  $\text{Ru}(0)$  ethene complexes.<sup>10</sup> A broad singlet was observed at  $\delta$  48.4 in the  $^{31}\text{P}\{^1\text{H}\}$  spectrum, while the proton spectrum exhibited a single broad resonance at  $\delta$  1.79 for the coordinated  $\text{C}_2\text{H}_4$  ligand. Cooling to 203 K resulted in sharpening of the  $^{31}\text{P}\{^1\text{H}\}$  NMR spectrum into a doublet and a triplet ( $J_{\text{PP}} = 9.7$  Hz), while decoalescence of the ethene signal in the  $^1\text{H}$  NMR spectrum led to the appearance of two broad peaks in a 1:1 ratio at 1.33 and 2.34 ppm. Although **1** proved to be stable in the solid state even under vacuum,  $^1\text{H}$  NMR spectroscopy indicated that, in the absence of an  $\text{C}_2\text{H}_4$  atmosphere, the complex released ethene into solution after only short periods of time.

An X-ray crystal structure study was carried out on **1** and is shown as an ORTEP<sup>11</sup> diagram in Figure 1. Selected geometric data are given in Table 1. The ruthenium exhibited a distorted-trigonal-bipyramidal geometry with the coordinated ethene ligand in the equatorial plane along with the CO and one  $\text{PPh}_3$  group. This is consistent with the well-established notion that the best  $\sigma$ -donor groups occupy axial positions and the best  $\pi$ -acceptors lie in the equatorial plane.<sup>12</sup> For this same reason, the Ru–P(3) bond length is longer than both the Ru–P(1) and Ru–P(2) distances. The two axial phosphines bend away from the equatorial  $\text{PPh}_3$  group (P(1)–Ru–P(3), 103.06(7)°; P(2)–Ru–P(3), 102.14(6)°) so that the (trans) P(1)–Ru–P(2) angle is only 153.79-

(10) (a) Ogasawara, M.; Macgregor, S. A.; Streib, W. E.; Folting, K.; Eisenstein, O.; Caulton, K. G. *J. Am. Chem. Soc.* **1996**, *118*, 10189. (b) Gottschalk-Gauding, T.; Huffman, J. C.; Gérard, H.; Eisenstein, O.; Caulton, K. G. *Inorg. Chem.* **2000**, *39*, 3957.

(11) McArdle, P. *J. Appl. Crystallogr.* **1994**, *27*, 438.

(12) Rossi, A. R.; Hoffmann, R. *Inorg. Chem.* **1975**, *14*, 365.

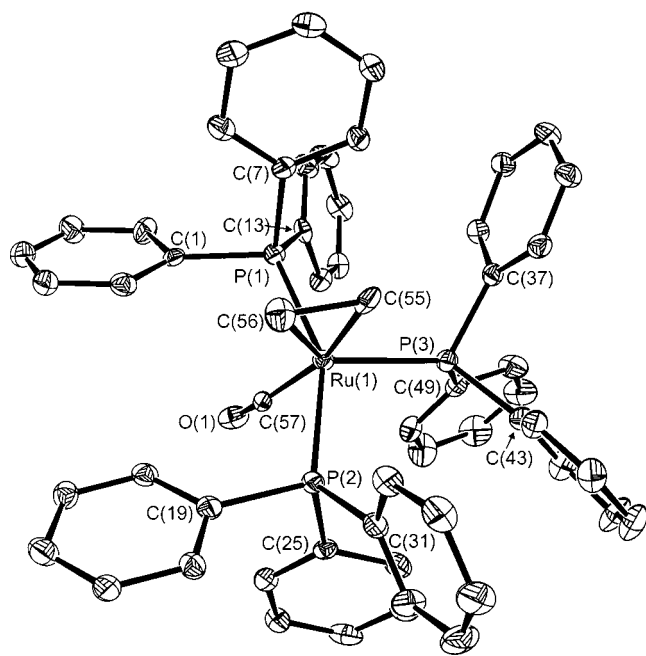
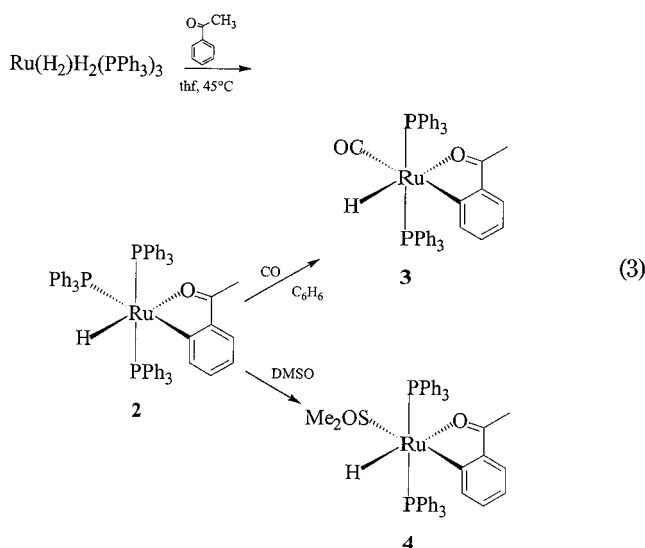


**Figure 1.** ORTEX diagram of  $\text{Ru}(\text{PPh}_3)_3(\text{CO})(\text{C}_2\text{H}_4)$  (**1**). Thermal ellipsoids are shown at the 30% probability level.

(7)°. The five atoms Ru, P(3), C(55), C(56), and C(57) define a good plane with a maximum deviation of 0.03 Å for C(55) from planarity. The C(55)–C(56) bond length of 1.451(11) Å is intermediate between C–C and C=C bond lengths and indicates some ruthenacyclop propane character to the structure.<sup>13</sup>

**Preparation and Characterization of  $\text{RuH}(\text{o}-\text{C}_6\text{H}_4\text{C}(\text{O})\text{CH}_3)(\text{L})(\text{PPh}_3)_3$  ( $\text{L} = \text{PPh}_3$ , **2**;  $\text{L} = \text{CO}$ , **3**;  $\text{L} = \text{DMSO}$ , **4**).** Reaction of the labile dihydrogen dihydride complex  $\text{Ru}(\text{H}_2)_2(\text{PPh}_3)_3$  with acetophenone at elevated temperatures gave the orange ortho-metallated complex  $\text{RuH}(\text{o}-\text{C}_6\text{H}_4\text{C}(\text{O})\text{CH}_3)(\text{PPh}_3)_3$  (**2**) in high yield (eq 3).<sup>14</sup> The IR spectrum of **2** showed two bands



at 1940 and 1574  $\text{cm}^{-1}$ , assigned to  $\nu_{\text{RuH}}$  and  $\nu_{\text{CO}}$ , respectively. The  $^{31}\text{P}\{^1\text{H}\}$  NMR spectrum displayed a doublet and a triplet ( $J_{\text{PP}} = 23.1$  Hz), while the proton spectrum showed a hydride signal at  $-15.42$  ppm split

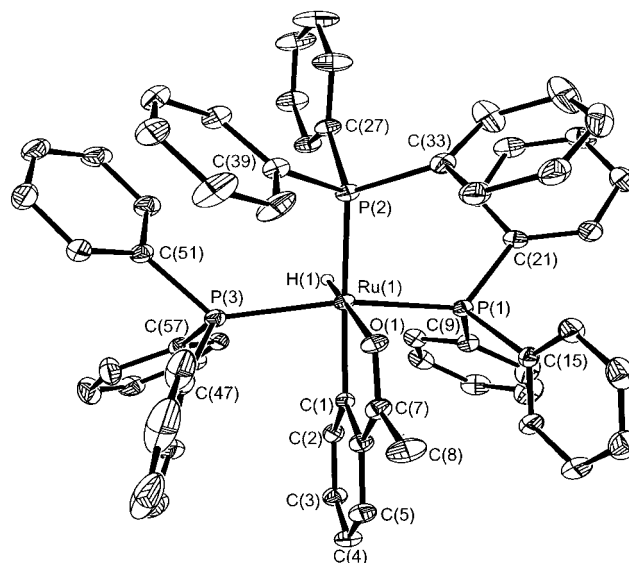


**Figure 2.** ORTEX diagram of  $\text{RuH}(\text{o}-\text{C}_6\text{H}_4\text{C}(\text{O})\text{CH}_3)(\text{PPh}_3)_3$  (**2**). Thermal ellipsoids are shown at the 30% probability level.

**Table 1. Selected Bond Lengths (Å) and Angles (deg) for  $\text{Ru}(\text{PPh}_3)_3(\text{CO})(\text{C}_2\text{H}_4)$  (**1**)**

|                   |            |                  |           |
|-------------------|------------|------------------|-----------|
| Ru(1)–C(57)       | 1.972(11)  | P(1)–C(7)        | 1.841(7)  |
| Ru(1)–C(55)       | 2.213(10)  | P(1)–C(1)        | 1.847(7)  |
| Ru(1)–C(56)       | 2.199(8)   | P(2)–C(25)       | 1.835(7)  |
| Ru(1)–P(1)        | 2.3498(19) | P(2)–C(31)       | 1.844(7)  |
| Ru(1)–P(2)        | 2.3825(19) | P(2)–C(19)       | 1.862(7)  |
| Ru(1)–P(3)        | 2.4148(18) | P(3)–C(37)       | 1.838(7)  |
| O(1)–C(57)        | 1.395(10)  | P(3)–C(49)       | 1.841(8)  |
| C(55)–C(56)       | 1.451(11)  | P(3)–C(43)       | 1.855(7)  |
| P(1)–C(13)        | 1.833(7)   |                  |           |
| C(57)–Ru(1)–C(55) | 164.6(3)   | C(55)–Ru(1)–P(2) | 96.30(18) |
| C(57)–Ru(1)–C(56) | 126.4(3)   | C(56)–Ru(1)–P(2) | 86.7(2)   |
| C(55)–Ru(1)–C(56) | 38.4(3)    | P(1)–Ru(1)–P(2)  | 153.79(7) |
| C(57)–Ru(1)–P(1)  | 83.4(2)    | C(57)–Ru(1)–P(3) | 104.6(2)  |
| C(55)–Ru(1)–P(1)  | 90.55(18)  | C(55)–Ru(1)–P(3) | 90.62(19) |
| C(56)–Ru(1)–P(1)  | 83.1(2)    | P(1)–Ru(1)–P(3)  | 103.06(7) |
| C(56)–Ru(1)–P(3)  | 129.0(2)   | O(1)–C(57)–Ru(1) | 176.5(9)  |
| C(57)–Ru(1)–P(2)  | 83.4(2)    | P(2)–Ru(1)–P(3)  | 102.14(6) |

into a doublet of triplets. The low solubility of this complex in standard NMR solvents (benzene, toluene, thf) prevented satisfactory  $^{13}\text{C}\{^1\text{H}\}$  NMR data from being recorded.

Crystals of **2** suitable for X-ray crystallography were slowly grown from a thf solution. An ORTEX plot of the asymmetric unit is shown in Figure 2, while selected bond lengths and angles are given in Table 2. The coordination geometry around the central ruthenium is distorted from an octahedron with a bent P(1)–Ru–P(3) angle of 158.8° arising due to the steric bulk of the equatorial  $\text{PPh}_3$  group. The Ru–O bond length in **2** (2.211(2) Å) is considerably longer than the Ru–O distances reported in the related complexes  $\text{RuCl}(\text{o}-\text{C}_6\text{H}_4\text{C}(\text{O})\text{CH}_3)(\text{CO})(\text{PPh}_3)_2$  and  $\text{RuCl}(\text{o}-\text{C}_6\text{H}_3\text{CH}_3\text{C}(\text{O})-\text{C}_6\text{H}_4\text{CH}_3)(\text{CO})(\text{PMe}_2\text{Ph})_2$  at 2.125(8) Å and 2.093(10)/

(13) (a) de C. T. Carrondo, M. A. A. F.; Chaudret, B. N.; Cole-Hamilton, D. J.; Skapski, A. C.; Wilkinson, G. *J. Chem. Soc., Chem. Commun.* **1978**, 463. (b) Wong, W.-K.; Chiu, K. W.; Statler, J. A.; Wilkinson, G.; Motevalli, M.; Hursthouse, M. B. *Polyhedron* **1984**, *3*, 1255. (c) Helliwell, M.; Vessey, J. D.; Mawby, R. J. *J. Chem. Soc., Dalton Trans.* **1994**, 1193.

(14) The benzophenone analogue,  $\text{RuH}(\text{o}-\text{C}_6\text{H}_4\text{C}(\text{O})\text{C}_6\text{H}_5)(\text{PPh}_3)_3$ , has been characterized in solution: Cole-Hamilton, D. J.; Wilkinson, G. *Nouv. J. Chim.* **1977**, *1*, 141.

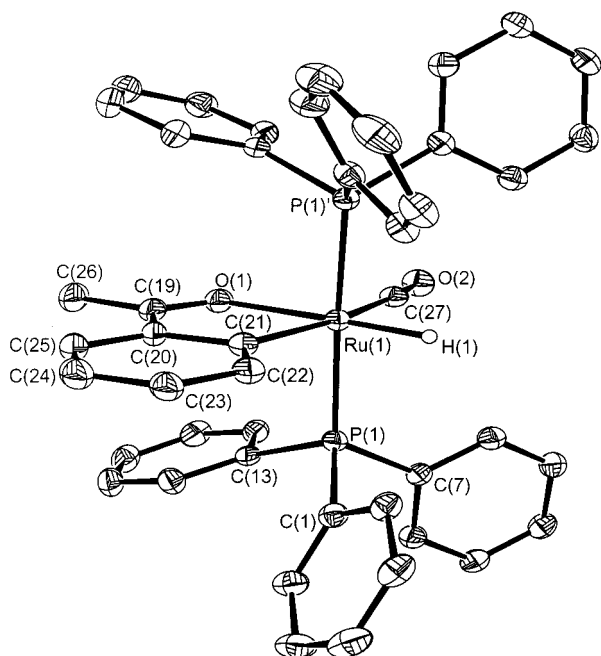


**Figure 3.** ORTEX diagram of  $\text{RuH}(\text{o}\text{-C}_6\text{H}_4\text{C}(\text{O})\text{CH}_3)(\text{CO})(\text{PPh}_3)_2$  (**3**). Thermal ellipsoids are shown at the 30% probability level.

**Table 2. Selected Bond Lengths (Å) and Angles (deg) for  $\text{RuH}(\text{o}\text{-C}_6\text{H}_4\text{C}(\text{O})\text{CH}_3)(\text{PPh}_3)_2$  (**2**)**

|                 |           |                 |           |
|-----------------|-----------|-----------------|-----------|
| Ru(1)–C(1)      | 2.115(3)  | C(7)–C(8)       | 1.507(5)  |
| Ru(1)–P(1)      | 2.3223(9) | Ru(1)–O(1)      | 2.211(2)  |
| Ru(1)–P(2)      | 2.3563(9) | Ru(1)–P(3)      | 2.3259(9) |
| O(1)–C(7)       | 1.251(4)  | C(1)–C(2)       | 1.417(5)  |
| C(1)–C(6)       | 1.428(4)  | C(2)–C(3)       | 1.377(5)  |
| C(3)–C(4)       | 1.394(5)  | C(4)–C(5)       | 1.373(5)  |
| C(5)–C(6)       | 1.401(5)  | C(6)–C(7)       | 1.448(5)  |
| C(1)–Ru(1)–O(1) | 76.68(10) | C(1)–Ru(1)–P(1) | 83.49(9)  |
| O(1)–Ru(1)–P(1) | 94.46(6)  | C(1)–Ru(1)–P(3) | 82.00(9)  |
| O(1)–Ru(1)–P(3) | 97.19(6)  | P(1)–Ru(1)–P(3) | 158.76(3) |
| C(1)–Ru(1)–P(2) | 168.12(9) | O(1)–Ru(1)–P(2) | 91.48(6)  |
| P(1)–Ru(1)–P(2) | 98.57(3)  | P(3)–Ru(1)–P(2) | 98.82(3)  |
| O(1)–C(7)–C(8)  | 118.5(3)  | O(1)–C(7)–C(6)  | 119.1(3)  |

2.136(11) Å, respectively.<sup>15,16</sup> This presumably reflects the fact that the chelated oxygen lies trans to a hydride rather than trans to a CO.

Addition of CO to a solution of  $\text{RuH}(\text{o}\text{-C}_6\text{H}_4\text{C}(\text{O})\text{CH}_3)(\text{PPh}_3)_3$  at room temperature led to rapid substitution of the equatorial phosphine ligand to afford  $\text{RuH}(\text{o}\text{-C}_6\text{H}_4\text{C}(\text{O})\text{CH}_3)(\text{CO})(\text{PPh}_3)_2$  (**3**) in good yield (eq 3). The proton NMR spectrum of this compound contained a triplet hydride signal at  $\delta$  –14.29, consistent with substitution of the equatorial  $\text{PPh}_3$  ligand. The  $^{13}\text{C}\{^1\text{H}\}$  NMR spectrum showed two low-field triplets at  $\delta$  202.9 ( $J_{\text{CP}} = 14.9$  Hz) and 204.9 ( $J_{\text{CP}} = 12.8$  Hz) assigned to the metalated carbon and carbonyl ligands, respectively, on the basis of  $^1\text{H}$ – $^{13}\text{C}\{^1\text{H}\}$  HMQC and HMBC experiments.

The molecular structure of **3** was confirmed by X-ray crystallography (Figure 3), although we were able to obtain crystals of only moderate quality. Selected bond distances and angles are given in Table 3. The presence of the relatively small CO ligand in an equatorial position relaxes the strain on the trans phosphine

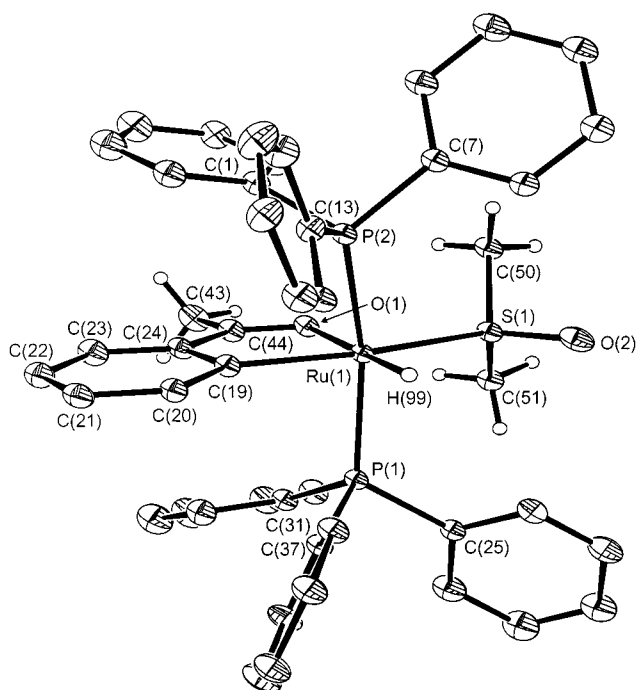


**Figure 4.** ORTEX diagram of  $\text{RuH}(\text{o}\text{-C}_6\text{H}_4\text{C}(\text{O})\text{CH}_3)(\text{DMSO})(\text{PPh}_3)_2$  (**4**). Thermal ellipsoids are shown at the 30% probability level.

**Table 3. Selected Bond Lengths (Å) and Angles (deg) for  $\text{RuH}(\text{o}\text{-C}_6\text{H}_4\text{C}(\text{O})\text{CH}_3)(\text{CO})(\text{PPh}_3)_2$  (**3**)**

|                    |           |                    |           |
|--------------------|-----------|--------------------|-----------|
| Ru(1)–C(27)        | 1.890(5)  | Ru(1)–C(21)        | 2.120(5)  |
| Ru(1)–O(1)         | 2.188(3)  | Ru(1)–P(1)         | 2.3191(8) |
| Ru(1)–P(1)#1       | 2.3191(8) | P(1)–C(13)         | 1.823(3)  |
| P(1)–C(1)          | 1.836(3)  | O(1)–C(19)         | 1.241(6)  |
| O(2)–C(27)         | 1.153(6)  | C(19)–C(26)        | 1.507(7)  |
| C(19)–C(20)        | 1.462(7)  | C(20)–C(21)        | 1.439(6)  |
| C(20)–C(25)        | 1.400(7)  | C(22)–C(23)        | 1.394(7)  |
| C(21)–C(22)        | 1.391(7)  | C(24)–C(25)        | 1.385(8)  |
| C(23)–C(24)        | 1.388(7)  |                    |           |
| C(27)–Ru(1)–C(21)  | 168.4(2)  | C(27)–Ru(1)–O(1)   | 91.42(17) |
| C(21)–Ru(1)–O(1)   | 76.94(16) | C(27)–Ru(1)–P(1)   | 92.97(2)  |
| C(21)–Ru(1)–P(1)   | 87.67(2)  | O(1)–Ru(1)–P(1)    | 92.82(2)  |
| C(27)–Ru(1)–P(1)#1 | 92.97(2)  | C(21)–Ru(1)–P(1)#1 | 87.67(2)  |
| O(1)–Ru(1)–P(1)#1  | 92.82(2)  | P(1)–Ru(1)–P(1)#1  | 171.70(4) |
| C(19)–O(1)–Ru(1)   | 116.2(3)  | O(1)–C(19)–C(20)   | 118.8(4)  |
| C(22)–C(21)–Ru(1)  | 132.8(4)  | C(20)–C(21)–Ru(1)  | 112.9(3)  |
| O(2)–C(27)–Ru(1)   | 173.7(4)  |                    |           |

groups relative to **2**, so that the P(1)–Ru–P(1) angle is opened out to 172°.

Substitution of  $\text{PPh}_3$  in **2** also occurred in the presence of DMSO to afford  $\text{RuH}(\text{o}\text{-C}_6\text{H}_4\text{C}(\text{O})\text{CH}_3)(\text{DMSO})(\text{PPh}_3)_2$  (**4**) in quantitative yield (eq 3). The NMR data are similar to those for **3**, apart from the coordinated DMSO, which was confirmed by the appearance of a singlet at  $\delta$  2.09 in the  $^1\text{H}$  NMR spectrum.<sup>17</sup> Red crystals of **4** suitable for X-ray crystallography were grown from toluene/hexane. An ORTEX plot is represented in Figure 4, while selected bond angles and distances are tabulated in Table 4. The sulfur-bound DMSO ligand occupies an equatorial site with a Ru–S bond distance of 2.308(11) Å, while the P–Ru–P angle of 157.7° is close to that found in **2**. The Ru–C bond lengths to the  $\text{sp}^2$  ortho-metalated carbon on the aromatic ring in **2–4** are all similar (2.100(5)–2.120(5) Å), apparently indepen-

(15) McGuiggan, M. F.; Pignolet, L. H. *Inorg. Chem.* **1982**, *21*, 2523.

(16) Dauter, Z.; Mawby, R. J.; Reynolds, C. D.; Saunders, D. R. *J. Chem. Soc., Dalton Trans.* **1985**, 1235.

(17) Complex **4** showed some evidence of decomposition in solution in the absence of DMSO.

**Table 4. Selected Bond Lengths (Å) and Angles (deg) for RuH(*o*-C<sub>6</sub>H<sub>4</sub>C(O)CH<sub>3</sub>)(DMSO)(PPh<sub>3</sub>)<sub>2</sub> (**4**)**

|                  |            |                  |            |
|------------------|------------|------------------|------------|
| Ru(1)–O(1)       | 2.183(3)   | Ru(1)–C(19)      | 2.100(5)   |
| Ru(1)–P(1)       | 2.3143(12) | Ru(1)–S(1)       | 2.3083(11) |
| S(1)–O(2)        | 1.477(4)   | Ru(1)–P(2)       | 2.3229(12) |
| S(1)–C(51)       | 1.802(5)   | S(1)–C(50)       | 1.788(5)   |
| O(1)–C(44)       | 1.244(6)   |                  |            |
| C(19)–Ru(1)–O(1) | 77.64(15)  | O(1)–Ru(1)–S(1)  | 86.78(9)   |
| C(19)–Ru(1)–S(1) | 164.41(14) | C(19)–Ru(1)–P(1) | 83.28(12)  |
| O(1)–Ru(1)–P(1)  | 96.55(9)   | S(1)–Ru(1)–P(1)  | 98.57(4)   |
| O(1)–Ru(1)–P(2)  | 98.20(9)   | C(19)–Ru(1)–P(2) | 83.59(12)  |
| P(1)–Ru(1)–P(2)  | 157.66(4)  | S(1)–Ru(1)–P(2)  | 98.93(4)   |
| C(44)–O(1)–Ru(1) | 114.6(3)   |                  |            |

**Table 5. Catalytic Coupling of 2'-Methylacetophenone with Triethoxyvinylsilane**

| catalyst precursor                                    | reacn time (min) | coupling product (%) | TON | TOF |
|---|------------------|----------------------|-----|-----|
| RuH <sub>2</sub> (CO)(PPh <sub>3</sub> ) <sub>3</sub> | 60               | 66                   |     |     |
|   | 120              | 96                   | 48  | 24  |
| <b>1</b>  | 120              | 44                   | 21  | 10  |
| <b>2</b>  | 30               | 62                   |     |     |
|   | 60               | 71                   |     |     |
|   | 120              | 76                   | 42  | 21  |
| <b>3</b>  | 120              | 4                    |     |     |
| <b>4</b>  | 30               | 12                   |     |     |
|   | 60               | 16                   |     |     |
|   | 240              | 22                   | 11  | 3   |
| <b>5</b>  | 120              | 4                    |     |     |
| <b>6</b>  | 600              | 0                    |     |     |

dent of the nature of the trans ligand (PPh<sub>3</sub>, CO, or DMSO).

**Catalytic Activity of 1–4 for Alkene–Ketone Coupling.** To assess the catalytic activity of complexes **1–4** relative to RuH<sub>2</sub>(CO)(PPh<sub>3</sub>)<sub>3</sub>, we chose to study the reaction of 2'-methylacetophenone with triethoxyvinylsilane, which were identified by Murai as the most reactive substrates.<sup>5</sup> Blocking of the second ortho position on the ketone by a methyl group also removed the potential for a double-insertion reaction. Table 5 summarizes these results and includes measurements on RuH<sub>2</sub>(CO)(PPh<sub>3</sub>)<sub>3</sub> which were performed for direct comparison. Although **1**, **2**, and **4** proved active for the reaction, lower yields of product were found in all cases compared with RuH<sub>2</sub>(CO)(PPh<sub>3</sub>)<sub>3</sub>. The carbonyl complex **3** showed essentially zero catalytic activity, in agreement with Chaudret's studies on RuH(*o*-C<sub>6</sub>H<sub>4</sub>C(O)CH<sub>3</sub>)(CO)(PCy<sub>3</sub>)<sub>2</sub>, which indicated that CO binds too strongly in the coordination site required for catalysis. The tris(phosphine) complex RuH(*o*-C<sub>6</sub>H<sub>4</sub>C(O)CH<sub>3</sub>)(PPh<sub>3</sub>)<sub>3</sub> produced a higher yield of product compared to RuH<sub>2</sub>(CO)(PPh<sub>3</sub>)<sub>3</sub> over shorter periods of time, although the catalytic activity ultimately plateaued off, leading to lower overall conversion after 2 h. It is not yet clear why this is the case. We assume that the poor activity of the ethene and DMSO complexes results from their instability in solution.

We also probed the effect of changing the PPh<sub>3</sub> ligands in RuH<sub>2</sub>(CO)(PPh<sub>3</sub>)<sub>3</sub> for AsPh<sub>3</sub> or the bidentate phosphine 1,2-bis(diphenylphosphino)propane (dppp). Neither RuH<sub>2</sub>(CO)(AsPh<sub>3</sub>)<sub>3</sub> (**5**) nor RuH<sub>2</sub>(CO)(PPh<sub>3</sub>)(dppp) (**6**) showed any activity for the Murai reaction. The latter has been reported to undergo rapid cyclometalation of one of the dppp phenyl rings upon heating to 120 °C.<sup>18</sup>

(18) Kawano, H.; Tanaka, R.; Fujikawa, T.; Hiraki, H.; Onishi, M. *Chem. Lett.* **1999**, 5, 401.

## Conclusions

We have prepared and characterized four new ruthenium complexes which have structural similarities to species proposed to be intermediates on the catalytic pathway for alkene insertion into aromatic ketone C–H bonds (Murai reaction). The tris(phosphine) cyclometalated complex RuH(*o*-C<sub>6</sub>H<sub>4</sub>C(O)CH<sub>3</sub>)(PPh<sub>3</sub>)<sub>3</sub> proved to be the most active of all of the catalyst precursors we have prepared for the reaction of 2'-methylacetophenone with CH<sub>2</sub>=CHSi(OEt)<sub>3</sub>. Substitution of the PPh<sub>3</sub> ligand in the equatorial coordination site by CO results in a complex with essentially zero catalytic activity. Thus, for ortho-metallated ketone compounds of this type with trans phosphine ligands, a weakly bound ligand must be present for activity to be observed. However, our results do not provide definitive evidence for or against the coordination of a CO ligand in metallated species on the Murai pathway.<sup>8,19</sup> It is possible, and indeed highly likely, that alternative isomers of **3** could be involved in the catalytic pathway which have activities different from those of the species we report. Further investigations to this end are currently in progress.

## Experimental Section

**General Comments.** All manipulations were carried out using standard Schlenk, high-vacuum, and glovebox techniques. All solvents were distilled from purple solutions of sodium benzophenone ketyl under a nitrogen atmosphere. C<sub>6</sub>D<sub>6</sub> and C<sub>6</sub>D<sub>5</sub>CD<sub>3</sub> (Goss Scientific Ltd.) were vacuum-transferred from potassium/benzophenone. Acetophenone, 2'-methylacetophenone, and triethoxyvinylsilane were purchased from Aldrich and dried over molecular sieves prior to use. Ethene (Aldrich, 99.9%) was used as received. RuH<sub>2</sub>(CO)(PPh<sub>3</sub>)<sub>3</sub>,<sup>5</sup> Ru(H<sub>2</sub>)<sub>2</sub>(PPh<sub>3</sub>)<sub>3</sub>,<sup>20</sup> RuH<sub>2</sub>(CO)(PPh<sub>3</sub>)(dppp),<sup>21</sup> and RuH<sub>2</sub>(CO)(AsPh<sub>3</sub>)<sub>3</sub><sup>22</sup> were prepared according to literature procedures. <sup>1</sup>H NMR spectra were recorded on JEOL EX 270, Bruker Avance 300, or Varian Mercury 400 MHz NMR spectrometers and referenced to the chemical shifts of residual protio solvent resonances (C<sub>6</sub>D<sub>5</sub>H, δ 7.15; C<sub>6</sub>D<sub>5</sub>CD<sub>2</sub>H, δ 2.10). <sup>13</sup>C NMR spectra were referenced to C<sub>6</sub>D<sub>6</sub> (δ 128.0) and C<sub>6</sub>D<sub>5</sub>-CH<sub>3</sub> (δ 21.1). <sup>31</sup>P NMR chemical shifts were referenced externally to 85% H<sub>3</sub>PO<sub>4</sub> (δ 0.0). IR spectra were recorded as Nujol mulls on a Nicolet Protégé 460 FTIR spectrometer. Elemental analyses were performed at the University of Bath.

**Ru(PPh<sub>3</sub>)<sub>3</sub>(CO)(C<sub>2</sub>H<sub>4</sub>) (**1**).** An ampule fitted with a Teflon stopcock containing a solution of RuH<sub>2</sub>(CO)(PPh<sub>3</sub>)<sub>3</sub> (0.2 g, 0.22 mmol) in 2 mL of toluene was freeze–pump–thaw–degassed and placed under 1 atm of ethene. The solution was heated at 120 °C for 10 min, during which time the solution turned deep red. The mixture was cooled rapidly to room temperature, and 20 mL of ethene-saturated diethyl ether was added. After the mixture was stirred for 15 min, a yellow precipitate formed. This was filtered off, washed with (2 × 10 mL) C<sub>2</sub>H<sub>4</sub>-saturated Et<sub>2</sub>O and (10 mL) hexane, and pumped to dryness to leave a yellow powder, typically in ca. 50% yield. Failure to use ethene-saturated solutions leads to depletion of product yields to between 0 and 30%. Recrystallization from hot ethene-saturated toluene gave thin red plates suitable for X-ray crystallography. Anal. Found (calcd) for RuC<sub>57</sub>H<sub>49</sub>P<sub>3</sub>O: C, 70.4 (72.52); H, 5.17 (5.23). Repeated analyses consistently gave a low percentage of carbon. <sup>1</sup>H NMR (C<sub>6</sub>D<sub>6</sub>, 400 MHz, 293 K):

(19) Trost, B. M.; Imi, K.; Davies, I. W. *J. Am. Chem. Soc.* **1995**, 117, 5371.

(20) Van Der Sluys, L. S.; Kubas, G. J.; Caulton, K. G. *Organometallics* **1991**, 10, 1033.

(21) Jung, C. W.; Garrou, P. E. *Organometallics* **1982**, 1, 658.

(22) Kim, J.-Y.; Jun, M.-J.; Lee, W. Y. *Polyhedron* **1996**, 15, 3787.

**Table 6. Crystal Data and Structure Refinement Details for Compounds 1–4**

|   | <b>1</b>  | <b>2</b>   | <b>3</b>   | <b>4</b>   |
|---|---|--|--|--|
| empirical formula   | C <sub>57</sub> H <sub>49</sub> O <sub>3</sub> P <sub>3</sub> Ru  | C <sub>68.2</sub> H <sub>65.4</sub> O <sub>1.8</sub> P <sub>3</sub> Ru | C <sub>45</sub> H <sub>38</sub> O <sub>2</sub> P <sub>2</sub> Ru | C <sub>48</sub> H <sub>50</sub> O <sub>3</sub> P <sub>2</sub> RuS <sub>2</sub> |
| fw  | 943.93  | 1107.79  | 773.76   | 902.01   |
| <i>T</i> /K   | 170(2)  | 150(2)   | 150(2)   | 150(2)   |
| cryst syst  | orthorhombic  | triclinic  | monoclinic   | triclinic  |
| space group   | <i>Pbca</i>   | <i>P</i> $\bar{1}$   | <i>P</i> <sub>2</sub> / <i>m</i>                                 | <i>P</i> $\bar{1}$   |
| <i>a</i> /Å   | 19.0110(5)  | 9.7870(1)  | 8.7830(6)  | 9.3177(3)  |
| <i>b</i> /Å   | 18.8250(4)  | 12.1770(2)   | 24.4420(8)   | 12.5569(4)   |
| <i>c</i> /Å   | 25.5770(7)  | 24.8940(4)   | 9.331(2)   | 20.0241(8)   |
| $\alpha$ /deg   |   | 91.170(1)  |  | 97.525(2)  |
| $\beta$ /deg  |   | 94.572(1)  | 114.977(7)   | 95.620(2)  |
| $\gamma$ /deg   |   | 111.824(1)   |  | 110.911(2)   |
| <i>V</i> /Å <sup>3</sup>  | 9153.5(4)   | 2741.36(7)   | 1815.8(4)  | 2143.05(13)  |
| <i>Z</i>  | 8   | 2  | 2  | 2  |
| <i>D</i> <sub>c</sub> /g cm <sup>-3</sup>                                   | 1.37  | 1.342  | 1.415  | 1.398  |
| $\mu$ /mm <sup>-1</sup>   | 0.488   | 0.420  | 0.558  | 0.579  |
| <i>F</i> (000)  | 3904  | 1156   | 796  | 936  |
| cryst size/mm   | 0.20 × 0.20 × 0.03  | 0.13 × 0.13 × 0.08   | 0.25 × 0.20 × 0.06   | 0.20 × 0.10 × 0.10   |
| $\theta$ range for data collectn/deg  | 3.05–23.82  | 3.54–25.00   | 3.66–27.69   | 3.61–24.98   |
| index ranges  | –21 ≤ <i>h</i> ≤ 21<br>–21 ≤ <i>k</i> ≤ 20<br>–29 ≤ <i>l</i> ≤ 29 | –11 ≤ <i>h</i> ≤ 11<br>–14 ≤ <i>k</i> ≤ 14<br>–29 ≤ <i>l</i> ≤ 29      | 0 ≤ <i>h</i> ≤ 11<br>–31 ≤ <i>k</i> ≤ 31<br>–12 ≤ <i>l</i> ≤ 11  | 0 ≤ <i>h</i> ≤ 11<br>–14 ≤ <i>k</i> ≤ 13<br>–23 ≤ <i>l</i> ≤ 23                |
| no. of rflns collected  | 55 531  | 36 392   | 24 744   | 15 221   |
| no. of indep rflns  | 7015 ( <i>R</i> (int) = 0.1551)                                   | 9605 ( <i>R</i> (int) = 0.0572)  | 4281 ( <i>R</i> (int) = 0.0966)                                  | 7186 ( <i>R</i> (int) = 0.1070)  |
| no. of rflns obsd (> 2 $\sigma$ ( <i>I</i> ))                               | 4947  | 8072   | 3306   | 5869   |
| no. of data/restraints/params   | 7015/0/560  | 9605/0/682   | 4281/0/249   | 7186/1/515   |
| goodness-of-fit on <i>F</i> <sup>2</sup>                                    | 0.984   | 1.028  | 1.017  | 0.990  |
| final <i>R</i> 1, <i>wR</i> 2 indices ( <i>I</i> > 2 $\sigma$ ( <i>I</i> )) | 0.0672, 0.1552  | 0.0448, 0.1154   | 0.0467, 0.1029   | 0.0589, 0.1653   |
| final <i>R</i> 1, <i>wR</i> 2 indices (all data)                            | 0.1048, 0.1795  | 0.0578, 0.1249   | 0.0696, 0.1141   | 0.0736, 0.1825   |
| largest diff peak, hole/e Å <sup>-3</sup>                                   | 1.172, –0.552   | 1.302, –0.821  | 0.545, –0.938  | 0.910, –1.099  |

$\delta$  8.00–6.60 (br, 45H, PC<sub>6</sub>H<sub>5</sub>), 1.79 (br s, 4H, C<sub>2</sub>H<sub>4</sub>). <sup>1</sup>H NMR (C<sub>6</sub>D<sub>5</sub>CD<sub>3</sub>, 400 MHz, 203 K):  $\delta$  2.34 (br s, 2H, C<sub>2</sub>H<sub>4</sub>), 1.33 (br s, 2H, C<sub>2</sub>H<sub>4</sub>). <sup>31</sup>P{<sup>1</sup>H} NMR (C<sub>6</sub>D<sub>6</sub>, 293 K):  $\delta$  48.4 (br s). <sup>31</sup>P{<sup>1</sup>H} NMR (C<sub>6</sub>D<sub>5</sub>CD<sub>3</sub>, 203 K):  $\delta$  45.6 (t, *J*<sub>PP</sub> = 9.7 Hz), 49.3 (d, *J*<sub>PP</sub> = 9.7 Hz). <sup>13</sup>C{<sup>1</sup>H} NMR (C<sub>6</sub>D<sub>6</sub>, 293 K):  $\delta$  214.1 (q, *J*<sub>CP</sub> = 13.7 Hz, Ru–CO), 29.8 (s, C<sub>2</sub>H<sub>4</sub>). <sup>13</sup>C{<sup>1</sup>H} NMR (C<sub>6</sub>D<sub>5</sub>CD<sub>3</sub>, 263 K):  $\delta$  213.4 (q, *J*<sub>CP</sub> = 13.0 Hz, Ru–CO), 29.4 (br s, C<sub>2</sub>H<sub>4</sub>), 25.7 (s, C<sub>2</sub>H<sub>4</sub>). <sup>13</sup>C{<sup>1</sup>H} NMR (C<sub>6</sub>D<sub>5</sub>CD<sub>3</sub>, 218 K):  $\delta$  213.3 (br t, *J*<sub>CP</sub> = 20.1 Hz, Ru–CO), 30.0 (br s, C<sub>2</sub>H<sub>4</sub>), 28.6 (s, C<sub>2</sub>H<sub>4</sub>). IR (cm<sup>-1</sup>): 1854 ( $\nu_{\text{CO}}$ ).

**RuH(*o*-C<sub>6</sub>H<sub>4</sub>C(O)CH<sub>3</sub>)(PPh<sub>3</sub>)<sub>3</sub> (2).** To a suspension of RuH<sub>2</sub>(H<sub>2</sub>)(PPh<sub>3</sub>)<sub>3</sub> (0.2 g, 0.22 mmol) in 5 mL of thf was added an excess of acetophenone (366  $\mu$ L, 3.1 mmol). The mixture was warmed with stirring to 45 °C for 12 h. The solution was concentrated to yield an orange precipitate, which was filtered off, washed with hexane (3 × 10 mL), and dried in vacuo. Yield: 0.183 g, 81%. Block-shaped orange crystals were formed when thf solutions were left at room temperature for 2 weeks. Anal. Found (calcd) for RuC<sub>62</sub>H<sub>53</sub>P<sub>3</sub>O.C<sub>4</sub>H<sub>4</sub>O: C, 72.8 (73.66); H, 5.48 (5.34). <sup>1</sup>H NMR (C<sub>6</sub>D<sub>6</sub>, 400 MHz, 293 K):  $\delta$  7.88–6.75 (m, 47H, PC<sub>6</sub>H<sub>5</sub>, *o*-C<sub>6</sub>H<sub>4</sub>), 6.30 (br t, *J*<sub>HH</sub> = 7.19 Hz), 6.45 (br t, *J*<sub>HH</sub> = 7.19 Hz), 1.36 (s, 3H, CH<sub>3</sub>), –15.42 (dt, *J*<sub>HP</sub> = 25.98 Hz, *J*<sub>HP</sub> = 13.19 Hz, 1H, Ru–H). <sup>31</sup>P{<sup>1</sup>H} NMR (C<sub>6</sub>D<sub>6</sub>, 293 K):  $\delta$  57.0 (d, *J*<sub>PP</sub> = 23.1 Hz), 46.6 (t, *J*<sub>PP</sub> = 23.1 Hz). <sup>13</sup>C{<sup>1</sup>H} NMR (C<sub>6</sub>D<sub>6</sub>, 293 K):  $\delta$  196.3 (s, Ru–O=C), 146.7 (s), 146.4 (s), 135.3–133.9 (m), 132.8 (s), 132.3 (s), 132.2 (s), 131.6 (s), 129.8 (s), 129.7 (s), 118.8 (s), 23.2 (s, CH<sub>3</sub>). IR (cm<sup>-1</sup>): 1940 ( $\nu_{\text{RuH}}$ ), 1574 ( $\nu_{\text{Ru–O=C}}$ ).

**RuH(*o*-C<sub>6</sub>H<sub>4</sub>C(O)CH<sub>3</sub>)(CO)(PPh<sub>3</sub>)<sub>2</sub> (3).** A benzene suspension (10 mL) of RuH(*o*-C<sub>6</sub>H<sub>4</sub>C(O)CH<sub>3</sub>)(PPh<sub>3</sub>)<sub>3</sub> (0.2 g, 0.20 mmol) was stirred under 1 atm of carbon monoxide for 30 min, during which time the color changed from red to yellow. The solution was concentrated and hexane added (10 mL) to give a yellow precipitate. This was filtered off, washed with 2 × 10 mL hexane, and dried in vacuo. Yield: 0.12 g, 76%. Anal. Found (calcd) for RuC<sub>45</sub>H<sub>38</sub>P<sub>2</sub>O<sub>2</sub>: C, 69.4 (69.85); H, 4.87 (4.95). <sup>1</sup>H NMR (C<sub>6</sub>D<sub>6</sub>, 400 MHz, 293 K):  $\delta$  7.60 (br, 10H, C<sub>6</sub>H<sub>5</sub>), 7.57 (br d, *J*<sub>HH</sub> = 7.60, 1H, C<sub>6</sub>H<sub>4</sub>), 6.90 (br, 20H, C<sub>6</sub>H<sub>5</sub>), 6.88 (br d, *J*<sub>HH</sub> = 7.60, 1H, C<sub>6</sub>H<sub>4</sub>), 6.56 (br t, *J*<sub>HH</sub> = 7.60, 1H, C<sub>6</sub>H<sub>4</sub>), 6.49 (br t, *J*<sub>HH</sub> = 7.60, 1H, C<sub>6</sub>H<sub>4</sub>), 1.66 (s, 3H, CH<sub>3</sub>), –14.29 (t, *J*<sub>HP</sub> = 21.18 Hz, 1H, Ru–H). <sup>31</sup>P{<sup>1</sup>H} NMR (C<sub>6</sub>D<sub>6</sub>, 293 K):  $\delta$  55.29

(s). <sup>13</sup>C{<sup>1</sup>H} NMR (C<sub>6</sub>D<sub>6</sub>, 293 K):  $\delta$  208.2 (s, Ru–O=C), 204.9 (t, *J*<sub>CP</sub> = 12.8 Hz, Ru–CO), 202.9 (t, *J*<sub>CP</sub> = 14.9 Hz, Ru–CO), 145.9 (s), 144.9 (s), 135.7 (t, *J*<sub>CP</sub> = 20.2 Hz), 134.4 (t, *J*<sub>CP</sub> = 5.9 Hz), 130.3 (s), 130.2 (s), 129.0 (s), 120.2 (s), 24.0 (s, CH<sub>3</sub>). IR (cm<sup>-1</sup>): 1932 ( $\nu_{\text{RuH}}$ ), 1899 ( $\nu_{\text{CO}}$ ), 1583 ( $\nu_{\text{Ru–O=C}}$ ).

**RuH(*o*-C<sub>6</sub>H<sub>4</sub>C(O)CH<sub>3</sub>)(DMSO)(PPh<sub>3</sub>)<sub>2</sub> (4).** DMSO (29  $\mu$ L, 0.40 mmol) was added to a toluene suspension (5 mL) of RuH(*o*-C<sub>6</sub>H<sub>4</sub>C(O)CH<sub>3</sub>)(PPh<sub>3</sub>)<sub>3</sub> (0.2 g, 0.20 mmol). The mixture was stirred for 30 min to give a homogeneous solution and then concentrated to ca. 1 mL. Addition of hexane (5 mL) and vigorous stirring for 5 min afforded a deep red oil. This operation was repeated twice more to give **4**, which was isolated as a light red powder upon drying in vacuo (0.162 g, 98%). Recrystallization from toluene/hexane afforded red needles suitable for X-ray diffraction. Anal. Found (calcd) for RuC<sub>46</sub>H<sub>44</sub>P<sub>2</sub>O<sub>2</sub>S·(CH<sub>3</sub>)<sub>2</sub>SO: C, 63.8 (63.91); H, 5.54 (5.62). <sup>1</sup>H NMR (C<sub>6</sub>D<sub>6</sub>, 400 MHz, 293 K):  $\delta$  7.80–6.90 (m, 30H, C<sub>6</sub>H<sub>5</sub>), 6.86 (br d, *J*<sub>HH</sub> = 7.59 Hz, 1H, C<sub>6</sub>H<sub>4</sub>), 6.74 (br d, *J*<sub>HH</sub> = 7.59 Hz, 1H, C<sub>6</sub>H<sub>4</sub>), 6.38 (br t, *J*<sub>HH</sub> = 7.20 Hz, 1H, C<sub>6</sub>H<sub>4</sub>), 6.12 (br t, *J*<sub>HH</sub> = 6.80 Hz, 1H, C<sub>6</sub>H<sub>4</sub>), 2.09 (s, 6H, CH<sub>3</sub>) 1.67 (s, 3H, CH<sub>3</sub>), –15.30 (t, *J*<sub>HP</sub> = 24.58 Hz, 1H, Ru–H). <sup>31</sup>P{<sup>1</sup>H} NMR (C<sub>6</sub>D<sub>6</sub>, 293 K):  $\delta$  58.04 (s). <sup>13</sup>C{<sup>1</sup>H} NMR (C<sub>6</sub>D<sub>6</sub>, 293 K):  $\delta$  206.4 (s, Ru–O=C), 195.2 (t, *J*<sub>CP</sub> = 15.8 Hz, Ru–C), 146.2 (s), 145.3 (s), 136.6 (t, *J*<sub>CP</sub> = 19.1 Hz), 133.8 (t, *J*<sub>CP</sub> = 5.8 Hz), 129.9 (s), 129.2 (s), 128.9–127.5 (m), 118.8 (s), 54.6 (s, CH<sub>3</sub>), 23.7 (s, CH<sub>3</sub>). IR (cm<sup>-1</sup>): 1971 ( $\nu_{\text{RuH}}$ ), 1571 ( $\nu_{\text{Ru–O=C}}$ ).

**Catalytic Reactions.** A 50 mL, three-necked, round-bottom flask equipped with an argon inlet, an outlet bubbler, and a reflux condenser was flame-dried under vacuum and flushed with argon. It was then charged with complexes **1–6** (0.04 mmol), 261  $\mu$ L (2 mmol) of triethoxyvinylsilane, 420  $\mu$ L (2 mmol) of 2'-methylacetophenone, 3 mL of toluene, and 200  $\mu$ L of dodecane as an internal reference. The solutions were stirred and heated to 135 °C. Two hundred microliter aliquots of solution were removed via syringe every 30 min over 4 h. The aliquots were diluted with hexane and passed through a short column of Celite to remove ruthenium residues. The formation of 2'-methyl-6'-[2-(triethoxysilyl)ethyl]acetophenone (retention time confirmed by an authentic sample) was analyzed by GC, as follows: Fisons GC 8000 series (equipped with a Supelco capillary column, 30 m × 0.32 mm) temperature program, 70

°C (0 min) → 8 °C/min → 200 °C (30 min); injection temperature, 270 °C; detector temperature, 270 °C.

**X-ray Experimental Data.** Crystallographic data for compounds **1–4** are summarized in Table 6. Data collections for all compounds were achieved using a Nonius Kappa CCD diffractometer and Mo K $\alpha$  radiation. The asymmetric unit in **2** consisted of one molecule of the ruthenium hydride complex plus 0.8 molecule of thf and 0.5 molecule of cyclohexane. In **3**, the asymmetric unit consisted of a half-molecule where the central metal, chelating ligand, hydride, and carbonyl moieties were all located on a mirror plane intrinsic in the space group symmetry. One molecule of free DMSO solvent was seen to be present in the asymmetric unit of **4** in addition to one molecule of the metal complex.

Full-matrix anisotropic refinement (SHELXL-97)<sup>23</sup> was implemented in the final least-squares cycles throughout. All data were corrected for Lorentz, polarization, and extinction. An absorption correction (multiscan) was applied to data for **1** and **2** (maximum and minimum transmission factors for these compounds were 1.035, 0.975; 1.020, respectively). Hydrogen atoms were included at calculated positions throughout, with the exception of the hydride in **2**, which was located and freely refined, and the hydride in **4**, which was located in refinement at a distance of 1.6 Å from the ruthenium atom.

(23) Sheldrick, G. M. *Acta Crystallogr.* **1990**, 467–473, A46. Sheldrick, G. M. SHELXL-97, A Computer Program for Crystal Structure Refinement; University of Göttingen, Göttingen, Germany, 1997.

The hydrogens on the alkene moiety of **1** could not be reliably located and, hence, were not included in the refinement. Some disorder was also evident in the positions of methyl hydrogens on C(26) in **3**.

Crystallographic data for the structural analyses have been deposited with the Cambridge Crystallographic Data Centre: CCDC 167070 for compound **1**, 167071 for compound **2**, 167072 for compound **3**, and 167073 for compound **4**.

**Acknowledgment.** We acknowledge the EPSRC for a project studentship (R.F.R.J.), the University of Bath for financial support, and Johnson Matthey plc for the loan of ruthenium trichloride hydrate. EPSRC/JREI is thanked for funding the X-ray diffractometer, as is Nicolet Instruments Ltd. for funding an IR spectrometer.

**Supporting Information Available:** X-ray crystallographic data, including tables of atomic coordinates, bond lengths and angles, anisotropic displacement parameters, hydrogen coordinates, and  $U_{eq}$  values and packing diagrams. This material is available free of charge via the Internet at <http://pubs.acs.org>.

OM010393Q